12-31-2010

Near minimum energy distributions on the sphere using Voronoi cells

Benedictus Sitou Mensah
Eastern Illinois University

THESIS MAINTENANCE AND REPRODUCTION CERTIFICATE

TO: Graduate Degree Candidates (who have written formal theses)

SUBJECT: Permission to Reproduce Theses

An important part of Booth Library at Eastern Illinois University's ongoing mission is to preserve and provide access to works of scholarship. In order to further this goal, Booth Library makes all theses produced at Eastern Illinois University available for personal study, research, and other not-for-profit educational purposes. Under 17 U.S.C. § 108, the library may reproduce and distribute a copy without infringing on copyright; however, professional courtesy dictates that permission be requested from the author before doing so.

By signing this form:

- You confirm your authorship of the thesis.
- You retain the copyright and intellectual property rights associated with the original research, creative activity, and intellectual or artistic content of the thesis.
- You certify your compliance with federal copyright law (Title 17 of the U.S. Code) and your right to authorize reproduction and distribution of all copyrighted material included in your thesis.
- You grant Booth Library the non-exclusive, perpetual right to make copies of your thesis, freely and publicly available without restriction, by means of any current or successive technology, including but not limited to photocopying, microfilm, digitization, or Internet.
- You acknowledge that by depositing your thesis with Booth LIbrary, your work is available for viewing by the public and may be borrowed through the library's circulation and interlibrary departmenst or accessed electronically.
- You waive the confidentiality provisions of the Family Educational Rights and Privacy Act (FERPA) (20 U.S.C. § 1232g; 34 CFR Part 99) with respect to the contents of the thesis, including your name and status as a student at Eastern Illinois Univerity.

Petition to Delay:

I respectfully petition that Booth Library delay maintenance and reproduction of my thesis until the date specified and for the reasons below. I understand that my degree will not be conferred until the thesis is available for maintenance and reproduction.

Date:

Reasons:

Author's Signature

2-14-12

Date

This form must be submitted in duplicate.

Near Minimum Energy Distributions on the Sphere using Voronoi Cells

(TITLE)

BY

Benedictus Sitou Mensah

THESIS

SUBMITTED IN PARTIAL FULFILLMENT OF THE REQUIREMENTS
FOR THE DEGREE OF

Master of Arts in Mathematics

IN THE GRADUATE SCHOOL, EASTERN ILLINOIS UNIVERSITY
CHARLESTON, ILLINOIS

2011

YEAR

I HEREBY RECOMMEND THAT THIS THESIS BE ACCEPTED AS FULFILLING
THIS PART OF THE GRADUATE DEGREE CITED ABOVE

2/15/2012	2/15/2012
THESIS COMMITTEE CHAIR — DATE	DEPARTMENT/SCHOOL CHAIR OR CHAIR'S DESIGNEE — DATE
2/15/2012	2/15/2012
THESIS COMMITTEE MEMBER — DATE	THESIS COMMITTEE MEMBER — DATE

Abstract

In this thesis we investigate the use of Voronoi cells to estimate a minimum energy configuration on the sphere. We introduce the notion of a Voronoi cell and give examples of its uses in various areas of mathematics. We consider the icosahedral decomposition of the sphere and apply a minimal energy configuration on the planar equilateral triangle to obtain spherical coordinates of a near minimal energy configuration on the sphere.

Dedications

I would like to dedicate this paper to my wife and kids for their never-ending support and love that they give me throughout my education and research. With their support I gained the strengths and the determination to thrive and overcome difficult times. Most importantly, I would also like to thank Dr. Coulton for his guidance, motivation, generosity, and his commitment for this research to be complete and make sense. Although my research journey has been long and rough, his patience throughout the entire process made this process comfortable. Lastly but not the least, I would like to give thanks to the Eastern Illinois University Department of Mathematics and Computer Science and the Department Chair, Dr. Andrews.

Acknowledgements

I am heartily thankful to my Mentor and Adviser, Dr. Coulton, whose encouragement, guidance and support from the initial to the final level enabled me to develop an understanding of the subject.

I offer my regards and gratitude to all of those who supported me in any respect during the completion of the project especially Dr. Andrews, Committee member and Department chair and Dr. Galperin, Committee member.

Table of Contents

Your Title Here

Your Name Here

EIU Math and C S.

List of Figures

Section 1. Basic Properties of Voronoi Diagrams

A *Voronoi diagram* with respect to a set of base points or sites is a collection of regions or cells that divide up the Euclidean plane such that all the points in a region are closer to the given base point than to any other base point and each region or cell corresponds to one of the base points. Points that are equidistant from base points are boundary points for each of the related base points.

Each of the bounded Voronoi cells are convex polygons since each boundary is determined by a pair of half planes which are in turn determined by two points. Some cells may be infinite or unbounded. For instance, consider the case of exactly two points.

The boundary between two adjacent cells is a line segment and the line that contains it is the perpendicular bisector of the segment joining the two sites. Voronoi cells constructed by points in general position meet in three boundary edges at a time. The intersection point is called a Voronoi point.

If three boundary edges in the plane meet at a Voronoi point, there is a circle centered at the point that passes through the three corresponding cell generating points or sites. If there were more than three sites, there would be more than three boundary edges. Note that for three points (sites) not on a line (i.e. in general position) there is a corresponding circumcenter (Voronoi point).

Given a set with a finite number of distinct points in Euclidean space which we shall call the base set, we associate all points in that space with the closest member of the base set with respect to the Euclidean distance. The result is a tessellation of the space into a set of Voronoi cells associated with the members of the base set.

Now consider a finite number of points with the Cartesian coordinates

$$P = \{(x_{11}, x_{12}), (x_{21}, x_{22}), \ldots, (x_{n1}, x_{n2})\}$$

or the equivalent location vectors $X_1, X_2, \ldots, X_n$ in two dimensional Euclidean space and assume that $2 \leq n < \infty$. We assume that the points are distinct such that: $X_i \neq X_j$, for $i \neq j$, with $i, j \in \{1, \ldots, n\}$. Let $p = (x_{01}, x_{02})$ be an arbitrary point in the space with location vector X. Then the Euclidean distance from point p to p_i is given by:

$$d(p, p_i) = ||XX_i|| = \sqrt{(x_{01} - x_{i1})^2 + (x_{02} - x_{i2})^2}.$$

If p_i is the nearest point from p, we have

$$||XX_i|| < ||XX_j||$$

for $j \neq i$ and $j \in \{1, \ldots, n\}$. We will call the open region $V(p_i)$ the Voronoi cell associated with the point p_i given by

$$V(p_i) = \{X \text{ s.t. } ||XX_i|| < ||XX_j||, \forall\ j \neq i\}.$$

We define V_P the Voronoi diagram generated by P as

$$V_P = \{V(p_1), V(p_2), \ldots, V(p_n)\}.$$

We define the Voronoi polygon by

$$\hat{V}(p_i) = \{X \text{ s.t. } ||XX_i|| \leq ||XX_j||,\ \forall\ j \neq i\}.$$

Note that this is a closed set containing the open Voronoi cell and the boundary of the open cell. We define the Voronoi polygon diagram as

$$\hat{V}_P = \{\hat{V}(p_1), \hat{V}(p_2), \ldots, \hat{V}(p_n)\}.$$

In the figure below we have a set of random points in a plane. We wish to apply the methods outlined above to create a Voronoi diagram model.

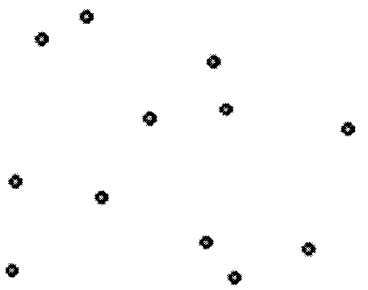

Figure 1. *A set of random points in the plane.*

The Voronoi diagram divides the plane into regions around the points that are shaped so that the borders of the cells are generated by the two nearest points.

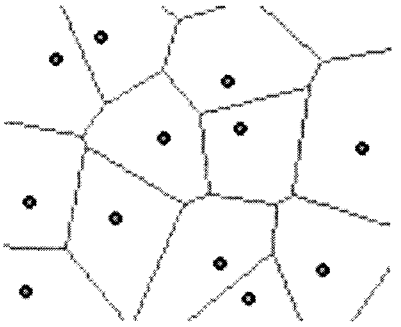

Figure 2. *An example of a portion of a Voronoi cell diagram.*

By drawing lines to mark out Voronoi cells, or drawing areas in the shape of those cells, we divide up the space into polygons which we will call tiles or tessellates. Every location within a Voronoi cell is closer to the base point about which that cell is drawn than it is to any other point.

Section 2. Applications of Voronoi Diagrams

Suppose we have a few hundred homes representing sampling sites scattered throughout a region (these are denoted by small dots in Figure 3 below). We also assume that there are a dozen post office collection and distribution centers, numbered 1 through 12, within the given region (these are denoted by the bigger dots in Figure 3 below).

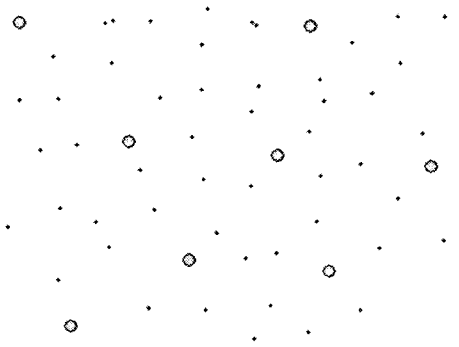

Figure 3. *The set of home sites and post offices.*

We would like to assign each home to the nearest post office. To do this, we first use a drawing of the post office site to create a Voronoi cell surrounding each post office (see figure 4 below).

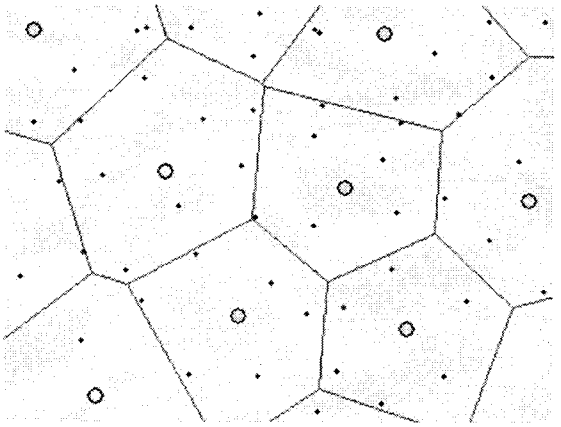

Figure 4. *A partial Voronoi diagram around post office sites.*

We can then assign a zip code to each cell, numbered from 1 to 12, and transfer the identification number of each home site to the Voronoi cell that encloses it. Thus each home has a zip code and the post office in that zip code is the closest to the homes in the region.

We can use this spatial layout to distribute mail into homes and/or pick up mail to transfer back to the post office closest to that home. Each home site will have a field that contains the data collection center or post office number that services it.

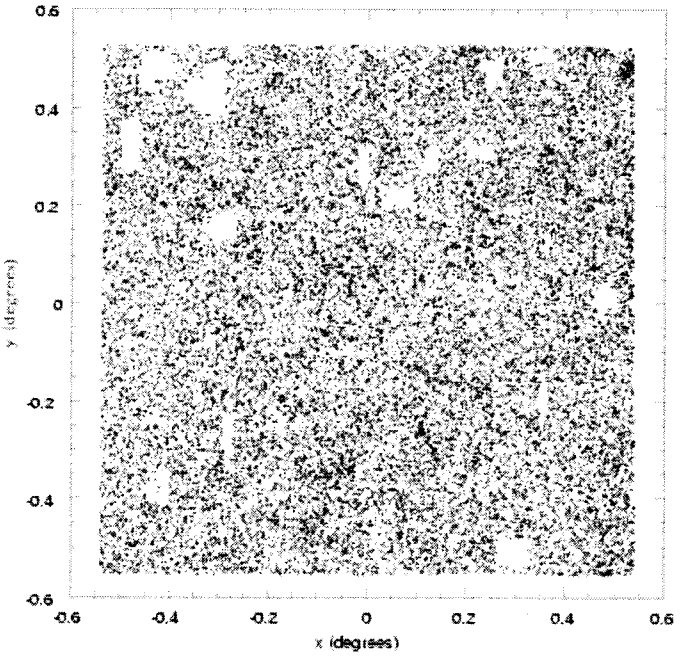

Figure 5. *Palomar Distant Cluster Survey.*

In Astronomy, we can decompose a star field by identifying galaxies as base points and

using these to construct a Voronoi diagram. The choice of base points can be varied by choosing base points depending on the brightness of the given galaxies in the star field. The Voronoi diagram gives a tessellation of the star field. The individual cells may then be studied and addressed in terms of the dominant galaxies in the star field.

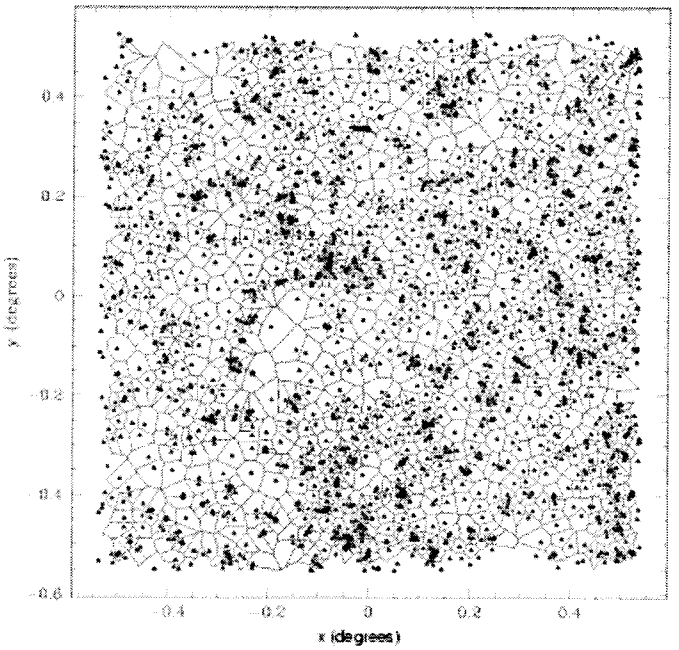

Figure 6. *Voronoi tessellation of a galaxy field.*

As a final example, consider the case of a robot in an enclosed space such as a room. Imagine that there are certain obstacles in the room which must be avoided. We represent these obstacles by base points. Note that the boundary of the Voronoi cells, in some sense, gives the optimally secure paths. For instance, if the cell boundaries are used as paths within the room, then these paths will be as far as possible from the obstacle base points.

The cell boundaries define the minimum approach distances for such paths. In addition, if the dimensions of the robot are known, then this information can be used to eliminate impassable boundary paths in the room.

Our research of Voronoi diagrams here will now be focused on the regular icosahedron. An icosahedron is any polyhedron having 20 faces, 30 edges and 12 vertices. A regular icosahedron has 20 equilateral triangles faces with five such triangles meeting at each of the twelve vertices. Tiling of surfaces with Voronoi cells in two dimensions is a feasible approach for embedding a uniform or a nearly uniform distribution of base points.

Tiling by nearly regular hexagons is equivalent to triangulating the surface by nearly

equilateral triangles. On flat surfaces, any rectangle constructed using equilateral triangles as packing cells has a regular hexagonal Voronoi cell tiling. If we let ρ denote the ratio of the height to base for the rectangle representation of the flat torus, then for any ratio ρ there is a point distribution using basic packing cells such that the cells make up a rectangular region of a torus representation in the plane. By slightly stretching the cell packing we may obtain a nearly regular hexagonal Voronoi cell tiling of the torus.

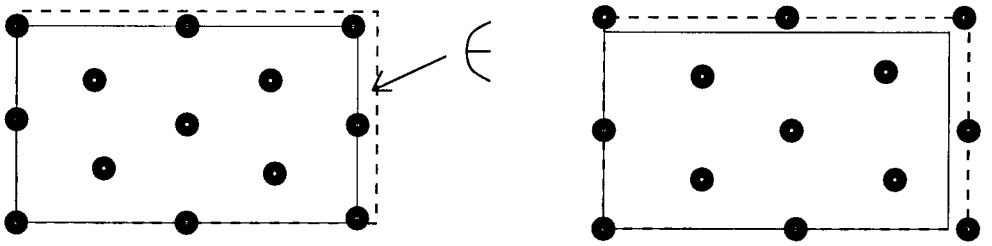

Figure 7. *Stretching a regular tiling to a near regular tiling.*

In the sphere, there can be no tiling by regular hexagons. It is a well known local result on the sphere that the ratio

$$\rho_1 = \frac{\sin(s)}{1-\cos(s)} = \frac{1+\cos(s)}{\sin(s)}, \ s \text{ is radial arc length,}$$

of the circumference of a circle to the area of that circle is smaller than the associated ratio $\rho_o = 2/r$ for the flat plane. This fact is due to the positive curvature of the sphere which is also related to the Euler characteristic. So in order to obtain even a local construction of a a near-hexagonal tiling we must shrink the circumference as we go out from the center. In other words, we must remove some area along boundaries as shown below.

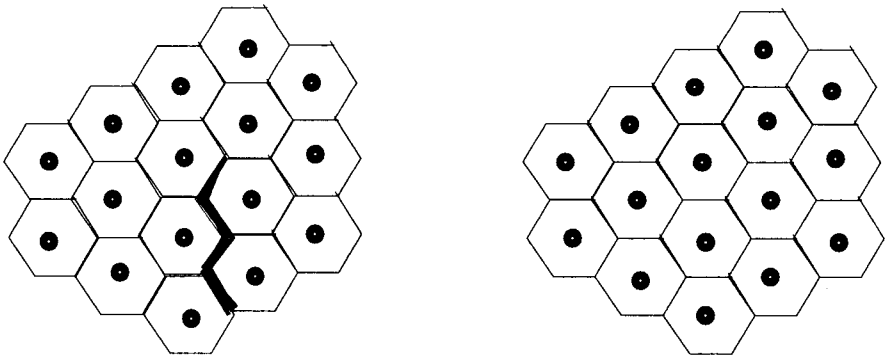

Figure 8. *A near-regular tiling for a portion of the sphere on the left after removing a strip from the tiling of a flat space on the right.*

The most regular tiling of a sphere with a large number of faces is by the regular icosahedron. We might then apply a near-equilateral triangular tiling of each equilateral triangle in the icosahedrons to obtain a near-regular-tiling of the sphere with many more faces. Of course this tiling might represent a near relative minimal energy configuration rather than an relative minimum energy configuration.

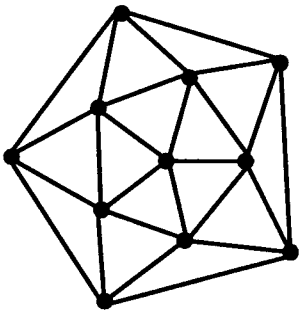

Figure 9. *A view of the icosahedron.*

Section 3. Simple Voronoi diagrams on Surfaces

We wish to consider the problem of minimal energy configurations as a set of points somehow evenly distributed on a closed and bounded surface. The simplest case is the flat torus $S^1 \times S^1$. This can be represented by a fundamental square domain in the covering space $\mathbf{R}^2$.

To model the minimal energy configuration we place base points on the surface and assume that the points interact with the nearby points according to Coulomb's law or some other appropriate force field relation.

It is well known that the integer lattice in the covering space determines a fundamental domain for the covering space. If we place one base point on each point of the lattice in the covering space, then this base point corresponds to a single point on the torus.

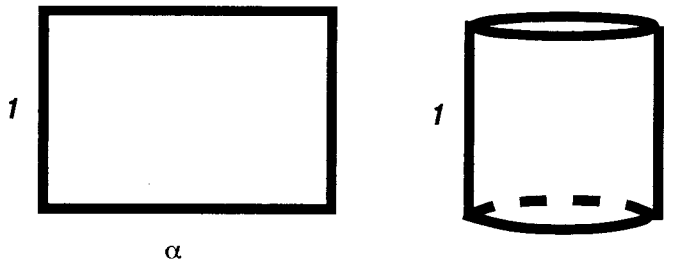

Figure 10. *A fundamental domain in* $\mathbf{R}^2$.

Now we can place new base points on the midpoints of the sides and diagonals of the fundamental domain, in this way we obtain a stable energy configuration for four points on the torus, i.e. we have placed five points on the fundamental domain that correspond to three new points on the torus.

Next, we can construct the Voronoi diagram for this distribution and note that the cells are all isomorphic and correspond to squares about each base point. Using the same procedure we can continue to construct stable minimal energy configurations, with similar Voronoi diagrams. It can be shown that for the next level eight points must be added. Of course, this does not solve the minimal energy configuration problem for intermediate numbers of points.

If we consider the unbounded case of $\mathbf{R^2}$ we observe that tessellations by regular polygons correspond to minimal energy. There are only three regular tesselations: by equilateral triangles; by squares; and by hexagons. It is easy to show that there are no regular tessellations for regular polygons with more than six sides since three interior angles for such polygons can not add up to 360^o.

On the other hand, it is well known that there are infinitely many different regular polygon tessellations in the hyperbolic plane. Each such tessellation corresponds to a minimal energy configuration and a corresponding Voronoi diagram.

Section 4. Voronoi diagrams on the Sphere

Following the work of others, Euclid demonstrated that there were five three dimensional regular solids with regular faces. These are usually referred to as the Platonic solids. The Platonic solids are

- The tetrahedron with four vertices and four faces each of which is an equilateral triangle
- The cube with eight vertices and six faces each of which is a square
- The octahedron with twelve vertices and eight faces each of which is an equilateral triangle
- The dodecahedron with twenty vertices and twelve faces each of which is a regular pentagon

- The icosahedron with twelve vertices and twenty faces each of which is an equilateral triangle.

Note that the number of vertices for the cube matches the number of faces for the octahedron and vice versa. The number of vertices for the dodecahedron matches the number of faces for the icosahedron and vice versa. The tetrahedron has the same number of vertices and faces. In this sense, the cube and the octahedron are dual to each other. The dodecahedron and the icosahedron are dual to each other and the tetrahedron is self dual.

If the tetrahedron is circumscribed by the sphere, then the vertices can be treated as base points. A Voronoi diagram will give a decomposition of the sphere into four identical Voronoi cells in the sense that each cell is an exact physical copy of the others. There are four intersection points for the boundaries of these Voronoi cells. These intersection points in turn determine a regular tetrahedron.

If the dodecahedron is circumscribed by the sphere and the vertices are taken as base points for a Voronoi diagram, then there are twenty identical regions which are precisely equilateral triangles on the sphere. Note that the base points here determine the dual Platonic solid. Five of these equilateral triangles meet at an intersection point. These intersection points determine an icosahedron. A similar result holds for each of the dual cases.

Observe that each of the Platonic solids corresponds to a minimal energy configuration on the sphere. But these are the only regular tessellations of the sphere.

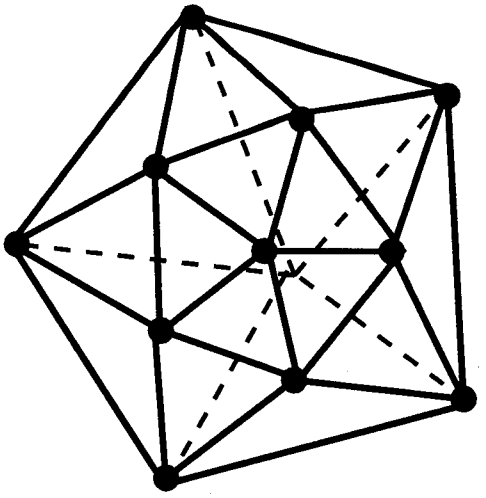

Figure 11. *A representation of the icosahedron with twenty faces*

Theorem A Assume that each face of the icosahedron is decomposed into k triangles. Let n denote the number of vertices inserted on each edge of a face. The total number of faces F on the icosahedrons is:

(1) $$F = 20(n+1)^2$$

The total Number of nodes N on the icosahedrons is:

(2) $$N = 20(n(n+2)/2) + 12 = 10n(n+2) + 12$$

and the number of new faces on each basic face is

(3) $$k = (n+1)^2$$

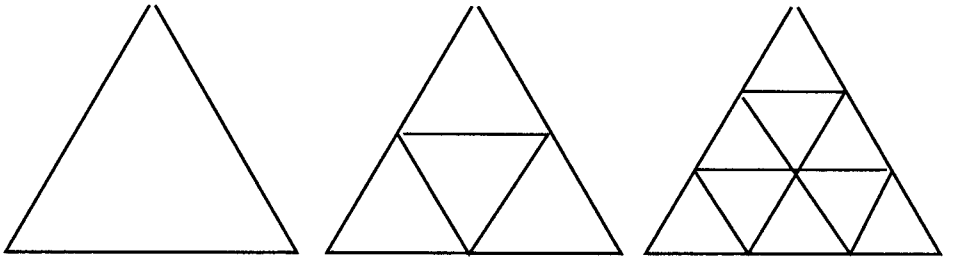

Figure 12. *Division of icosahedron faces.*

Proof: If $n = 0, F = 20(0+1)^2 = 20(1)^2 = 20$. Let assume that (1) is true at n and prove that is true at $n+1$. For n, we have $F = 20(n+1)^2$ and for $n+1$, we will add $n+2$ triangles touching the side and $n+1$ triangles whose vertex touches the side. This gives $F = 20((n+1)^2 + 2(n+1) + 1)$. Therefore, F has an increment of $2(n+1)+1$ to the previous step on each initial face of the icosahedrons. We now have,

$$F = 20((n^2 + 2n + 1) + 2n + 2 + 1)$$

$$= 20(n^2 + 2n + 2n + 1 + 2+)$$

$$= 20(n^2 + 4n + 4)$$

$$= 20(n+2)^2$$

$$= 20((n+1)+1)^2$$

Therefore, the total number of new faces on the icosahedron tiling of the sphere for n divisions of the edge is $F = 20(n+1)^2$. For (2) we consider $n = 0$, which gives

$$N = 10(0)(0+2) + 12 = 0 + 12 = 12.$$

This is true, since an icosahedrons has 12 vertices. If $n = 1$, we have no interior vertices on the basic face triangle and one node inserted on each edge. The basic icosahedron has 30 basic edges and so we should have $H = 42$ vertices. According to (2) we for $n = 1$ we have

$$N = 10(1)(3) + 12 = 42.$$

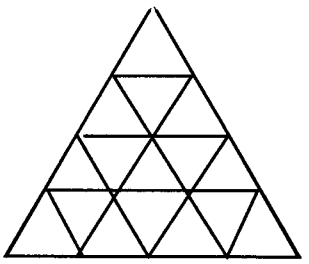

Figure 13. *Additional vertices on a basic face.*

For n new vertices on each edge, we have an $0 + 1 + 2 + 3 + \ + (n - 1)$ new interior vertices on each basic face which gives a total of

$$20(0 + 1 + 2 + 3 + \ldots + (n - 1)) + 30n$$

$$= 20((n - 1)n/2) + 30n$$

$$= 10n^2 - 10n + 30n$$

$$= 10n(n + 2)$$

new nodes. This gives the total number of nodes as

$$N = 10n(n + 2) + 12.$$

Now that we know how the number of faces and nodes on the icosahedrons increase, we can find the coordinates of each point on the surface of the sphere at any division step.

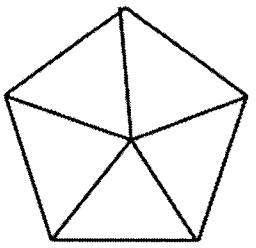

Figure 14. *Pentagons formed on the north and south parts of the icosahedron hemisphere.*

In figure 14, each of the interior angles formed by the center lines joining the edging point measures 72 degrees. Using spherical polar coordinates, the position of point P is described as (r, ϕ, θ), where r is the distance from the origin of the sphere, ϕ is the horizontal angle measured on the xy plane from the x axis in the counterclockwise direction, and θ is the angle measured from the z axis. The relationship between the spherical coordinates and the Cartesian coordinates can be described as:

$$x = r\cos\phi\sin\theta$$

$$y = r\sin\phi\sin\theta$$

$$z = r\cos\theta$$

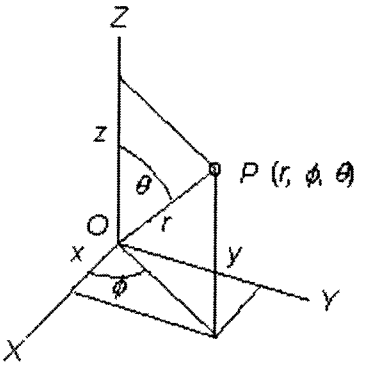

Figure 15. *Polar coordinate representation.*

The angle θ formed by the z axis and a pair of the points on first triangle with one edge (point B below) in the x direction in the upper hemisphere is obtained as follow:

$$A = (x\cos(72^o), x\sin(72^o), \sqrt{1-x^2}), \quad B = (x, 0, \sqrt{1-x^2}).$$

The Euclidean distance is

$$||AB|| = \sqrt{x^2(1-\cos(72^o))^2 + x^2\sin^2(72^o)}$$

$$= \sqrt{1 + x^2 - 2x^2\cos(72^o)}.$$

On the other hand, if s is the arc-length between the points on the sphere then

$$\frac{||AB||}{2} = \sin(s/2).$$

Thus

$$\sin^2(s/2) = (1-\cos^2(s/2)) = \frac{1}{2} - \frac{\cos(s)}{2} = \frac{1-\sqrt{1-x^2}}{2}$$

and so

$$\frac{||AB||}{2} = \sqrt{\frac{1-\sqrt{1-x^2}}{2}}.$$

By solving this equation

$$1 + x^2 - 2x^2\cos(72^o) = 2(1 - \sqrt{1-x^2})$$

we obtain $x \approx 0.830152$. Therefore, $s = \arcsin(0.830152)180/\pi \approx 56.04^o$. We can then write the polar coordinates of each of the 12 points components that constitute the icosahedrons. The angles ϕ and θ are given in degrees. The north pole point $N = (1, 0, 0)$ The south pole point $S = (1, 0, 180)$ Other interior points are:

$$(1, 0, 56.04), (1, 72, 56.04), (1, 144, 56.04), (1, 216, 56.04), (1, 288, 56.04), (-1, 36, 56.04),$$

$$(-1, 108, 56.04), (-1, 180, 56.04), (-1, 252, 56.04), (-1, 324, 56.04).$$

From the twelve vertices of the icosahedrons, we have chosen three on a face with vertex at the north pole to obtain a representation of all the vertices. We can then find the components of the vectors needed to obtain the coordinates of the interior points gained through subdivision of the edges. The calculation of the vector coordinates of the vertices at different edge divisions are obtained in the maple worksheets that follow.

This particular study of icosahedrons can be applied in various fields. This study showed us that for n divisions of the edges of icosahedrons, the total number of faces on the icosahedrons is (1):

$$F = 20(n+1)^2$$

As we divide the edges of the icosahedrons into smaller edges, the number of base points or vertices increases. Likewise, the number of edges increase. We found and proved the relationship between n the number of edge divisions and N the number of vertices, namely:

$$N = 10n(n+2) + 12.$$

Finally, the maple sheets below compile the coordinates of the vertices for a division of the edge into n new points. We apply a force function for an added weight to each point to obtain a relation to be minimized. This force function can be used in other applications to express the star brightness of a site, or in the case of the post office example to indicate the population concentration near the site of the post office.

The maple worksheet calculates the first vertex vector, B, in the icosahedron representation along with the Euclidean distance, DE, between vertices. This is used to find the base points for the near minimal energy configuration for $n = 14$, that is 14 new points along an edge.

All the new basis points are listed in the body of the worksheet.

Appendix A

```
> restart:
> Digits := 20;
> with(linalg);
```

$$Digits := 20$$

```
Warning, the protected names norm and trace have been redefined and
unprotected
```

[*BlockDiagonal, GramSchmidt, JordanBlock, LUdecomp, QRdecomp, Wronskian, addcol, addrow, adj, adjoint, angle, augment, backsub, band, basis, bezout, blockmatrix, charmat, charpoly, cholesky, col, coldim, colspace, colspan, companion, concat, cond, copyinto, crossprod, curl, definite, delcols, delrows, det, diag, diverge, dotprod, eigenvals, eigenvalues, eigenvectors, eigenvects, entermatrix, equal, exponential, extend, ffgausselim, fibonacci, forwardsub, frobenius, gausselim, gaussjord, geneqns, genmatrix, grad, hadamard, hermite, hessian, hilbert, htranspose, ihermite, indexfunc, innerprod, intbasis, inverse, ismith, issimilar, iszero, jacobian, jordan, kernel, laplacian, leastsqrs, linsolve, matadd, matrix, minor, minpoly, mulcol, mulrow, multiply, norm, normalize, nullspace, orthog, permanent, pivot, potential, randmatrix, randvector, rank, ratform, row, rowdim, rowspace, rowspan, rref, scalarmul, singularvals, smith, stackmatrix, submatrix, subvector, sumbasis, swapcol, swaprow, sylvester, toeplitz, trace, transpose, vandermonde, vecpotent, vectdim, vector, wronskian*] (1)

```
> va := [0.89442719,0,0.447213595]:vamag := sqrt(va[1]^2 + va[3]^2):
> DE := sqrt(va[1]^2 + (1-va[3])^2);
> vnp := [0,0,1]:
> vc := [0.89442719*cos(2.0*3.1415/5), 0.8944*sin(2*3.1415/5),
  0.447213595]: vacmag := sqrt((va[1]-vc[1])^2 + (va[2] - vc[2])^2 +
  (va[3]-vc[3])^2):
> vmp := va + (1/3)*(vnp -va + vc -va):
> vmps := normalize(vmp);
> v :=crossprod(vc-va,vnp-va);sqrt(dotprod(v,v));
```

$$DE := 1.0514622236505314055$$

$$vmps := [0.49113616134235766847 \quad 0.35680655617653458902 \quad 0.79465360534721987974]$$

$$v := [0.47020824447029750881 \quad 0.34162335919949975797 \quad 0.76081291980471415404]$$

$$0.95741245639502931752 \tag{2}$$

```
> f := (x,y) -> (-v[1]*x -v[2]*y +v[3])/v[3];
```

$$f := (x, y) \rightarrow \frac{-v_1 x - v_2 y + v_3}{v_3} \tag{3}$$

```
> parts := 15; v1 :=(vc-va)/DE;
> v2 :=(vnp-va)/DE;
> pt := (i,j) ->va + (DE/parts)*(i*v1 + j*v2);
```

$$parts := 15$$

$$v1 := [-.58775526881297891453, 0.80898265790228581551, 0.]$$

$$v2 := [-.85065080787655167556, 0., 0.52573111288848976576]$$

$$pt := (i, j) \rightarrow va + \frac{DE\,(i\,v1 + j\,v2)}{parts} \tag{4}$$

```
> for k from 0 to parts do
> for m from 0 to parts-k do
```

Figure 16.

```
> spt := (m,k) -> pt(m,k)/sqrt(pt(m,k)[1]^2 + pt(m,k)[2]^2 +pt(m,k)
  [3]^2);
> od; od;
> phi := arcsin(0.89442719);evalf(2*Pi/5);
```

$$\phi := 1.1071487155582106318$$

$$1.2566370614359172954 \tag{5}$$

```
> for k from 1 to parts -1 do
> spt(0,k) :=[sin((1 -k/parts)*phi),0,cos((1 -k/parts)*phi)];
> pt(0,k) := [v[3]*spt(0,k)[1]/(v[1]*spt(0,k)[1]  + v[3]*spt(0,k)[3]
  ),0,v[3]*spt(0,k)[3]/(v[1]*spt(0,k)[1] + v[3]*spt(0,k)[3])];
> vtp := pt(0,k) - va: vcmult:= sqrt(vtp[1]^2 + vtp[3]^2)/DE:
> pt(k,0) := va + [(vc[1]-va[1])*vcmult,(vc[2]-va[2])*vcmult,(vc[3]
  -va[3])*vcmult];
> spt(k,0) := pt(k,0)/sqrt(pt(k,0)[1]^2 + pt(k,0)[2]^2 +pt(k,0)[3]
  ^2);
> spt(parts-k,k) := [cos(1.256637062)*sin((1 -k/parts)*phi),sin
  (1.256637062)*sin((1 -k/parts)*phi),cos((1 -k/parts)*phi)];
> od:
> euv := (i,j) -> 6*spt(i,j)-spt(i-1,j)-spt(i-1,j+1)-spt(i+1,j)-spt
  (i+1,j-1)-spt(i,j+1) -spt(i,j-1);
```

$$euv := (i,j) \to 6\,spt(i,j) - spt(i-1,j) - spt(i-1,j+1) - spt(i+1,j) - spt(i + 1,j-1) - spt(i,j+1) - spt(i,j-1) \tag{6}$$

```
> :
> eud1 := (i,j) -> dotprod(euv(i,j),spt(i,j));
> eud1(2,2);
> force := (i,j) -> matadd(euv(i,j),- eud1(i,j)*spt(i,j));
> spt2 := (i,j) -> spt(i,j); pt2 := (i,j) -> pt(i,j);
```

$$eud1 := (i,j) \to (linalg{:}\text{-}dotprod)(euv(i,j), spt(i,j))$$

$$0.017565507022604671661$$

$$force := (i,j) \to (linalg{:}\text{-}matadd)(euv(i,j), -eud1(i,j)\,spt(i,j))$$

$$spt2 := (i,j) \to spt(i,j)$$

$$pt2 := (i,j) \to pt(i,j) \tag{7}$$

```
> change:=0.2;
```

$$change := 0.2 \tag{8}$$

```
> for k from 1 to parts -1 do
> for m from 1 to parts - k do
> pt2(k,m) := spt(k,m) - [force(k,m)[1]*change,force(k,m)[2]*change,
  force(k,m)[3]*change];
> spt2(k,m) := pt2(k,m)/sqrt(pt2(k,m)[1]^2 + pt2(k,m)[2]^2 + pt2(k,
  m)[3]^2); print(k,m,spt2(k,m));
> od;
> od;
```

1, 1, [0.84676381977944508996, 0.067747224695596198305, 0.52763751483245373663]

1, 2, [0.80819920947839170983, 0.063846925103079847079, 0.58543796251471805995]

1, 3, [0.76241938537084975688, 0.065699795836130376713, 0.64373924661917768872]

1, 4, [0.71079717823396455269, 0.067254767380366280793, 0.70017438376396379566]

1, 5, [0.65355927523099396255, 0.068433421514026410476, 0.75377525866760940585]

1, 6, [0.59119726097939091576, 0.069170071625955468799, 0.80355541178049826979]

1, 7, [0.52446462159363454022, 0.069420792863768940924, 0.84859743943451268086]

Figure 17.

1, 8, [0.45433420712579733969, 0.06917011639409130123 1, 0.88814183733984795520]
1, 9, [0.38192040394465009360, 0.06843350836677728357 4, 0.92165810362811302342]
1, 10, [0.30838073348351068293, 0.06725489138382486929 8, 0.94888255479860197108]
1, 11, [0.23481736391238675655, 0.06569995054177756539 7, 0.96981664354868941769]
1, 12, [0.16219759504019339525, 0.06384710338643140794 8, 0.98469055421098651353]
1, 13, [0.09325126841500802135 4, 0.06774922959450726755 6, 0.99333490969981663479]
1, 14, [0.02319874010837322461 6, 0.06103886118568931793 3, 0.99786576045204512540]
2, 1, [0.83116458045626513774, 0.13451994710541138498, 0.53950887298145345682]
2, 2, [0.79170220938392481649, 0.13057384379077256805, 0.59678981473741238126]
2, 3, [0.74290444646475262495, 0.13408913430525743793, 0.65583007515984362173]
2, 4, [0.68710570969717135121, 0.13691827227961324599, 0.71353985902506678287]
2, 5, [0.62468214622874941778, 0.13890589609235766143, 0.76842525219686948164]
2, 6, [0.55646090011559556566, 0.13993239194674991727, 0.81900561190177588055]
2, 7, [0.48369166209040254226, 0.13993245586104670995, 0.86397990938500419418]
2, 8, [0.40794195997497425423, 0.13890608367204519968, 0.90237933110786135818]
2, 9, [0.33093434166216145063, 0.13691857175843287478, 0.93366791002811200798]
2, 10, [0.25436305671307339636, 0.13408952825009863582, 0.95776794360285822156]
2, 11, [0.17973254737311649777, 0.13057431166667809943, 0.97501105662835621273]
2, 12, [0.11084829894996164400, 0.13452346039295677335, 0.98469086175500000052]
2, 13, [0.04172526786536014535 8, 0.12509998727681563988, 0.99126635936306469059]
3, 1, [0.80703904782892126791, 0.20300954192193077061, 0.55450437434526696712]
3, 2, [0.76447293171570250415, 0.20046199126036963472, 0.61269578645027937262]
3, 3, [0.71161438717267030573, 0.20538908492890825862, 0.67187817925642636083]
3, 4, [0.65171912463027024093, 0.20913705756244261371, 0.72905683848742400355]
3, 5, [0.58540365560886160738, 0.21148568470591499561, 0.78267257851815127078]
3, 6, [0.51375407181697928926, 0.21228620357163900815, 0.83125887752529580327]
3, 7, [0.43825495555854718338, 0.21148595100484246316, 0.87361678466931552330]
3, 8, [0.36064258201921662437, 0.20913757275608854346, 0.90895456635422893997]
3, 9, [0.28271436921343367436, 0.20538981722045283123, 0.93695656698824587694]
3, 10, [0.20614064003926636130, 0.20046289952041250285, 0.95776858501418317031]
3, 11, [0.13505286572734500263, 0.20301468434508261162, 0.96981738559333848993]
3, 12, [0.06347149926967508136 9, 0.19172283714313820164, 0.97939456936325991781]
4, 1, [0.77748998001690964088, 0.27248863939112841551, 0.56679738211822840687]
4, 2, [0.73113487185717724297, 0.27240801008421285600, 0.62548834936899376214]
4, 3, [0.67420832605572177498, 0.27834176401123519604, 0.68408259405151905247]
4, 4, [0.61042570428692127435, 0.28251754157980607822, 0.73997587679972290159]
4, 5, [0.54066432821706437769, 0.28467642422744222026, 0.79160685803160386233]
4, 6, [0.46625782198364575593, 0.28467665844497978590, 0.83759348348448080777]

Figure 18.

4, 7, [0.38887985044104987256, 0.28251822853457498591, 0.87690131284348773256]
4, 8, [0.31036296397466009404, 0.27834285941028100027, 0.90895549022390110993]
4, 9, [0.23249604614167916282, 0.27240944851371692330, 0.93366947089906436672]
4, 10, [0.15926580444714676100, 0.27249544734077192085, 0.94888388895183366588]
4, 11, [0.08580982710134412506 6, 0.26019344761893565273, 0.96173595305000926023]
5, 1, [0.74247848450997641824, 0.34206169610926864400, 0.57595094938251387214]
5, 2, [0.69166533994631219742, 0.34502933002015276912, 0.63447129087358782675]
5, 3, [0.63088024570461856065, 0.35142689790828764227, 0.69172917460971536575]
5, 4, [0.56366003860362919220, 0.35543865304343687537, 0.74562103296783584692]
5, 5, [0.49113610526844517560, 0.35680661554241656500, 0.79465361334792210010]
5, 6, [0.41484707728039276454, 0.35543936865602598315, 0.83759462610580393287]
5, 7, [0.33658320574142506982, 0.35142828177494623531, 0.87361885761557054068]
5, 8, [0.25818608121888494183, 0.34503129571271468701, 0.90238204350687330153]
5, 9, [0.18311360726345663042, 0.34207010112003665668, 0.92166016120622923432]
5, 10, [0.10843337018176327679, 0.32958624238729118807, 0.93787798410030418632]
6, 1, [0.70218342151885461693, 0.41070097480896255473, 0.58160394757518835468]
6, 2, [0.64641870826421969861, 0.41675182200714715433, 0.63910935876400742965]
6, 3, [0.58222395897410953662, 0.42298124032783260832, 0.69433574870320678941]
6, 4, [0.51224961029032803399, 0.42620154714911727402, 0.74562227566315762590]
6, 5, [0.43784311325524135394, 0.42620205566428387712, 0.79160925709752571113]
6, 6, [0.36067813207682952870, 0.42298273199285166099, 0.83126222906940294715]
6, 7, [0.28257338906318112768, 0.41675420118952549137, 0.86398392090607136357]
6, 8, [0.20619318864244579912, 0.41071079160423209710, 0.88814470364760144431]
6, 9, [0.13097560774297647686, 0.39879167818543486396, 0.90764012008416778407]
7, 1, [0.65701913920211579908, 0.47731935314989147476, 0.58351699703665871011]
7, 2, [0.59613997869757073480, 0.48595762505765443522, 0.63911056355436972281]
7, 3, [0.52920971988606893420, 0.49136994009250660878, 0.69173163463267669272]
7, 4, [0.45735069274753834789, 0.49321460949368301180, 0.73997952189593770231]
7, 5, [0.38206105534918488118, 0.49137126754880581699, 0.78267721789569611704]
7, 6, [0.30506350469560630550, 0.48596019431077061387, 0.81901095697693315891]
7, 7, [0.22810504513277944388, 0.47733028059778344418, 0.84860113811461151911]
7, 8, [0.15303465300199045651, 0.46658784021531124051, 0.87113499662438746504]
8, 1, [0.60762053461266405740, 0.54086189803792459437, 0.58160613233341511937]
8, 2, [0.54191207016193689872, 0.55115605842449081895, 0.63447482808601890431]
8, 3, [0.47309242231012400414, 0.55516488640439802886, 0.68408735469699417337]
8, 4, [0.40032321001400103656, 0.55516572059483690056, 0.72906265176629471028]
8, 5, [0.32517195936540869789, 0.55115850787339831730, 0.76843184215727950247]
8, 6, [0.24849005856182120546, 0.54087353579573681148, 0.80355989762541067080]

Figure 19.

```
    8, 7, [0.17420736144806614892, 0.53174245690268426755, 0.82879536361179036245]
    9, 1, [0.55479459981024502911, 0.60039866577456846989, 0.57595520151962174139]
    9, 2, [0.48504335117384823040, 0.61113844794769669759, 0.62549400070833881391]
    9, 3, [0.41527036896261571624, 0.61328715613120853336, 0.67188494906951715191]
    9, 4, [0.34257460243317830869, 0.61114042164288399055, 0.71354749442619991294]
    9, 5, [0.26706226527932350012, 0.60041054526705028530, 0.75378042134032613909]
    9, 6, [0.19412722633970663672, 0.59312770234092343797, 0.78135404824537079705]
   10, 1, [0.49944714952077381351, 0.65519947897965470529, 0.56680348232907216124]
   10, 2, [0.42692139125369841172, 0.66508110805196629013, 0.61270322783740522874]
   10, 3, [0.35712951705897215531, 0.66508225099457329505, 0.65583847665200059191]
   10, 4, [0.28363055415369937108, 0.65521110324840371389, 0.70018006179159019004]
   10, 5, [0.21249782120913788040, 0.64982310472707468503, 0.72977709510797514303]
   11, 1, [0.44250034709412324231, 0.70477645629534940409, 0.55451202824947801807]
   11, 2, [0.36886816739947041374, 0.71257815748317982509, 0.59679866333398640121]
   11, 3, [0.29810545019620585808, 0.70478734103000122232, 0.64374524812784302553]
   11, 4, [0.22911452405427024664, 0.70118420462555665533, 0.67516460663382726921]
   12, 1, [0.38481797068796965851, 0.74888966773174268392, 0.53951774298926718920]
   12, 2, [0.31049145611572926746, 0.74889937631483994366, 0.58544408770981530491]
   12, 3, [0.24387108089805004183, 0.74686569629124886665, 0.61864248771403079322]
   13, 1, [0.32611936130278459202, 0.78437135288221671130, 0.52764357568455707450]
   13, 2, [0.25675223255148495506, 0.78680184048569448986, 0.56126745397194727474]
   14, 1, [0.26986836532014895442, 0.82008826935262303257, 0.50460508902472460015]   (9)
> force(5,5);
    [2.80369554197965 10^-7   -2.968294158853709 10^-7   -4.0003524476823 10^-8]   (10)
> for k from 1 to parts -1 do
> for m from 1 to parts - k do
> spt(k,m) :=spt2(k,m);
> od;
> od;
> euv := (i,j) -> 6*spt2(i,j)-spt2(i-1,j)-spt2(i-1,j+1)-spt2(i+1,j)-
  spt2(i+1,j-1)-spt2(i,j+1) -spt2(i,j-1);
> eud1 := (i,j) -> dotprod(euv(i,j),spt2(i,j));
> eud1(2,2);
> force := (i,j) -> matadd(euv(i,j),- eud1(i,j)*spt2(i,j));
> force(3,2);
euv := (i,j)→6 spt2(i,j) − spt2(i − 1,j) − spt2(i − 1,j + 1) − spt2(i + 1,j) − spt2(i
    + 1,j − 1) − spt2(i,j + 1) − spt2(i,j − 1)
                    eud1 := (i,j)→ (linalg:-dotprod)(euv(i,j), spt2(i,j))
                                0.018003077204452379102
              force := (i,j)→ (linalg:-matadd)(euv(i,j), −eud1(i,j) spt2(i,j))
 [0.010408312236660176015   −0.019000158602144020014   −0.006770184215164358521]   (11)
> :
```

Figure 20.

References

[1] M. Atiyah and P. Sutcliffe, *The geometry of point particles*, Royal Soc. London Proc. Ser. A Math. Phys. Eng. Sci. **458** (2002), 10891115.

[2] T. Erber and G. M. Hockney, *Complex systems: equi- librium configurations of N equal charges on a sphere 2 N 112* , Advances in chemical physics, Vol. XCVIII, 495594, Adv. Chem. Phys., XCVIII, Wiley, New York, 1997.

[3] D. P. Hardin and E. B. Saff, *Discretizing manifolds via minimum energy points*, Notices of the American Mathematical Society, November, 2004.

[4] E. A. Rakhmanov, E. B. Saff, and Y. M. Zhou, Minimal discrete energy on the sphere, Math. Res. Lett. 1 (1994), 647662.